

1 **Thermal transport in organic semiconducting polymers - supporting information**

2 John C. Duda,<sup>1,2</sup> Patrick E. Hopkins,<sup>1, a)</sup> Yang Shen,<sup>3</sup> and Mool C. Gupta<sup>3, b)</sup>

3 <sup>1)</sup>*Department of Mechanical and Aerospace Engineering, University of Virginia,*  
4 *Charlottesville, Virginia, USA 22904*

5 <sup>2)</sup>*Seagate Technology, Bloomington, Minnesota, USA 55431*

6 <sup>3)</sup>*Department of Electrical and Computer Engineering, University of Virginia,*  
7 *Charlottesville, Virginia, USA 22904*

---

<sup>a)</sup>Electronic mail: phopkins@virginia.edu

<sup>b)</sup>Electronic mail: mgupta@virginia.edu

8 The extremely low thermal conductivities of PCBM thin films<sup>1</sup> create a situation in which  
9 our TDTR signal at the 11.39 MHz modulation frequency is proportional to  $\sqrt{\kappa C}$ , where  $\kappa$  is  
10 thermal conductivity and  $C$  is the volumetric heat capacity, i.e., we are in an effusivity regime.<sup>2</sup>  
11 As a result, uncertainties in the assumed heat capacities directly propagate to uncertainties in the  
12 measured thermal conductivities. The higher conductivities of the other polymeric thin films yield  
13 thermal penetration depths on the order of the film thicknesses and we are therefore less sensitive  
14 to the heat capacities of those films.<sup>3,4</sup> The heat capacities of P3HT films are well documented  
15 in the literature<sup>5,6</sup> and a 25% variation in the assumed PEDOT:PSS heat capacity corresponded  
16 to uncertainties in thermal conductivities less than 15% due to the aforementioned diminished  
17 sensitivity to heat capacity. However, heat capacity of PCBM remains an unknown.

18 As we had discussed previously,<sup>1</sup> we assumed that the heat capacities of PCBM thin films were  
19 the same as  $C_{60}/C_{70}$  fullerite microcrystals<sup>7</sup> due to the fact that the separation distance between  
20 fullerene moieties in both PCBM films processed via chlorobenzene solution and fullerite micro-  
21 crystals are nearly identical. While PCBM thin films would then have higher atomic densities  
22 than the fullerite microcrystals, many of the additional modes contributed by the molecular tail  
23 (e.g., C-H stretching) are likely to be “frozen-out” near room temperature. If the presence of the  
24 molecular tail does not significantly disturb the lower frequency vibrations of the fullerene moiety,  
25 the heat capacities near room temperature should be similar. Still, the validity of this assumption  
26 may come into question. As our reports suggest PCBM thin films exhibit lower conductivities  
27 than any other previously measured fully dense solid, we use this opportunity to further address  
28 this assumption with both experimental and computational techniques.

29 To study the effect of a molecular tail on the vibrational spectra of an isolated  $C_{60}$  fullerene  
30 molecule we implemented classical molecular dynamics simulations using the LAMMPS package<sup>8</sup>  
31 and the ReaxFF interatomic potential.<sup>9</sup> Isolated fullerene and PCBM molecules were first con-  
32 structed in Avagadro<sup>10</sup> and a energy minimization procedure was run to determine the quasi-  
33 equilibrium positions of the atoms. The molecules were then imported into LAMMPS where a  
34 subsequent energy minimization procedure was run (now with interatomic interactions specified  
35 by the ReaxFF interatomic potential) to generate our initial conditions. The molecules were heated  
36 to 100 K using a NVT scheme for 1e6 time steps using a time step of 0.1 fs, after which a set  
37 number of time steps were run using an NVE scheme. During the NVE portion of the simulation,  
38 velocities of all atoms were recorded every 20 time steps to construct velocity fluctuation time se-  
39 ries. These time series were then used to calculate the density of vibrational states of the isolated

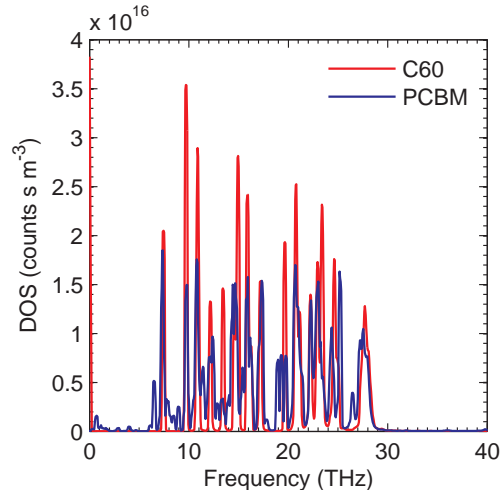


FIG. 1. Vibrational spectra from simulated molecules generated from the molecular dynamics velocity fluctuation time series. Here, only the vibrational spectra of the carbon atoms of the fullerene moiety within PCBM are plotted, thus isolating how the molecular tail distorts the vibrational modes of the carbon cage.

40 molecules,<sup>11,12</sup> the results of which are shown in Figs. 1 and 2.

41 In Fig. 1 we plot the vibrational spectra of an isolated  $C_{60}$  fullerene as well as the vibrational  
 42 spectra of the fullerene moiety belonging to an isolated PCBM molecule, i.e., we ignore the vi-  
 43 brations of the atoms within the molecular tail. This, then, allows us to isolate how the presence  
 44 of the molecular tail affects the vibrational modes of the carbon cage. Generally, the molecu-  
 45 lar tail broadens the sharp peaks seen in the vibrational spectra of the isolated  $C_{60}$  fullerene but  
 46 does not shift them to higher or lower frequencies. This is in agreement with a previous study of  
 47 poly-ethylene-oxide functionalized  $C_{60}$  fullerenes.<sup>13</sup> In Fig. 2, the vibrational spectra of an iso-  
 48 lated  $C_{60}$  fullerene is compared to the total vibrational spectra of an isolated PCBM molecule,  
 49 i.e., the vibrations within the tail are included. The molecular tail adds a significant number of  
 50 modes outside the range of frequencies exhibited by  $C_{60}$ . This could be expected since the tail in-  
 51 creases the length of the molecule (adding lower frequency modes) while contributing additional  
 52 stiff interatomic interactions between carbon and lighter atoms (C-H stretching modes).

53 Since the simulated molecules were isolated, these vibrational spectra do not lend insight into  
 54 the zone center modes that are associated with long-wavelength, distributed vibrations. However,  
 55 we were able to measure the sound speed of PCBM as discussed in Ref. 1 and found it to be lower  
 56 than that of fullerite microcrystals as reported in Ref. 7, indicating the distribution of zone center  
 57 modes is across a lower frequency range in PCBM relative to that of the fullerite compacts. Thus,

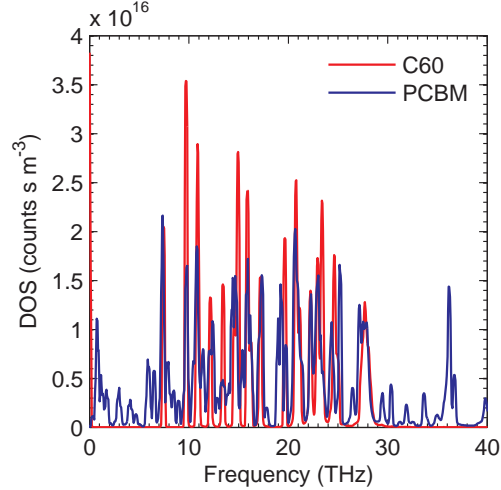


FIG. 2. Vibrational spectra from simulated molecules generated from the molecular dynamics velocity fluctuation time series. Here, the vibrational spectra of the all atoms of the PCBM molecule are plotted, including those within the molecular tail. However, many vibrational modes contributed by the tail are at frequencies higher than the range plotted here, e.g., C-H stretching modes.

58 both computational and experimental results suggest that PCBM thin films exhibit lower frequency  
 59 modes than fullerene-based films. In turn, near room temperature where high-frequency modes  
 60 are frozen out due to Bose-Einstein statistics, the volumetric heat capacity of a PCBM film should  
 61 be slightly higher than that of a fullerene film. By taking the heat capacity of PCBM to be that of  
 62 fullerite microcrystals, we are thus erring on the side of caution: by ignoring the molecular tail,  
 63 we are underestimating the specific heat, and thus overestimating the conductivity.

64 To further explore this assumption, we turn to discussions from previous works demonstrating  
 65 the ability to measure the thermal conductivity of thin films with TDTR while maintaining little  
 66 to negligible sensitivity to heat capacity.<sup>3,4</sup> In this case, the modulation frequency can be tuned so  
 67 that the thermal penetration depth is on the same order as a film thickness, as previously discussed.  
 68 We measured a variety of PCBM films, both annealed and annealed at varying thicknesses and  
 69 frequencies, as show in Figs. 2 and 3 of the main text. We found that the thermal conductivities  
 70 of the PCBM films ranged from  $0.0314 \pm 0.002$  to  $0.057 \pm 0.005 \text{ W m}^{-1} \text{ K}^{-1}$ , and varied based on  
 71 both the substrate and annealing condition. However, we did not observe any general trend based  
 72 on these parameters at this time, and this will be addressed in a future study focused solely on  
 73 PCBM processing and thermal transport.

74 By fitting the TDTR data over multiple frequencies, we can estimate the effective volumet-

75 ric heat capacities of the thin PCBM films,<sup>3</sup> and found that our experimentally fit heat capacities  
76 ranged from  $1.2 - 1.8 \text{ MJ m}^{-3} \text{ K}^{-1}$ . Interestingly, there was no apparent correlation between the  
77 heat capacities measured by TDTR and the measured thermal conductivities. For example, the  
78 highest heat capacity was measured on a film that also had a high conductivity ( $1.8 \text{ MJ m}^{-3} \text{ K}^{-1}$   
79 and  $0.054 \text{ W m}^{-1} \text{ K}^{-1}$ , respectively); if our sensitivity to effusivity was skewing our measure-  
80 ments, one would expect films with the highest heat capacities to have the lower thermal con-  
81 ductivities and vice versa. We speculate that substrate and processing conditions may change the  
82 packing densities of PCBM, although further work is required to say this with certainty.

83 We conclude that within our experimental uncertainties PCBM films can exhibit the lowest  
84 thermal conductivities of any fully dense solid reported to date. Clearly, more work is necessary to  
85 determine the correlation between the thermal conductivity of PCBM films and various processing  
86 and structural conditions. However, TDTR or its variations could prove effective tools to determine  
87 both density and thermal transport properties of these materials.

## 88 REFERENCES

- 89 <sup>1</sup>J. C. Duda, P. E. Hopkins, Y. Shen, and M. C. Gupta, *Physical Review Letters* **110**, 015902  
90 (2013).
- 91 <sup>2</sup>A. J. Schmidt, R. Cheaito, and M. Chiesa, *Review of Scientific Instruments* **80**, 094901 (2009).
- 92 <sup>3</sup>J. Liu, J. Zhu, M. Tian, X. Gu, A. Schmidt, and R. Yang, *Review of Scientific Instruments* **84**,  
93 034902 (2013).
- 94 <sup>4</sup>D. G. Cahill, A. Melville, D. G. Schlom, and M. A. Zurbuchen, *Applied Physics Letters* **96**,  
95 121903 (2010).
- 96 <sup>5</sup>J. A. Malen, K. Baheti, T. Tong, Y. Zhao, J. A. Hudgings, and A. Majumdar, *Journal of Heat*  
97 *Transfer* **133**, 081601 (2011).
- 98 <sup>6</sup>P. S. O. Patrício, H. D. R. Calado, F. A. C. de Oliveira, A. Righi, B. R. A. Neves, G. G. Silva,  
99 and L. A. Cury, *Journal of Physics: Condensed Matter* **18**, 7529 (2006).
- 100 <sup>7</sup>J. R. Olson, K. A. Topp, and R. O. Pohl, *Science* **259**, 1145 (1993).
- 101 <sup>8</sup>S. Plimpton, *Journal of Computational Physics* **117**, 1 (1995).
- 102 <sup>9</sup>K. Chenoweth, A. C. T. van Duin, and W. A. Goddard, *The Journal of Physical Chemistry A*  
103 **112**, 1040 (2008), pMID: 18197648, <http://pubs.acs.org/doi/pdf/10.1021/jp709896w>.
- 104 <sup>10</sup>M. Hanwell, D. Curtis, D. Lonie, T. Vandermeersch, E. Zurek, and G. Hutchison, *Journal of*

105 Cheminformatics **4**, 17 (2012).

106 <sup>11</sup>L. V. Zhigilei, D. Srivastava, and B. J. Garrison, Surface Science **374**, 333 (1997).

107 <sup>12</sup>J. C. Duda, T. S. English, E. S. Piekos, W. A. Soffa, L. V. Zhigilei, and P. E. Hopkins, Physical  
108 Review B **84**, 193301 (2011).

109 <sup>13</sup>H. Kim, D. Bedrov, G. D. Smith, S. Shenogin, and P. Keblinski, Physical Review B **72**, 085454  
110 (2005).